

STATISTICS OF INTERNAL EXCITATIONS OF ATOMIC SYSTEMS

R. S. Berry^{a*}, *B. M. Smirnov*^b

^a *Department of Chemistry, University of Chicago
Chicago, IL 60637, USA*

^b *Institute of High Temperatures
127412, Moscow, Russia*

Submitted 6 June 2001

The character of internal excitations is compared for phase transitions and chemical transitions in atomic systems. Although the temperature dependences of some physical parameters of atomic systems have resonance-like structures with maxima in both cases, the dependences of the partition functions on the number of elementary excitations or the excitation energy differ because of the difference in the numbers of interactions that govern the transitions. The phase changes of condensed rare gases are considered in the case where the external pressure is small and the differences between phases are predominantly associated with differences in configurations. Important energy parameters of rare gases are determined by the attractive part of the pairwise interaction potential between atoms. The statistical analysis shows the existence of a «freezing limit» temperature for these systems, below which the liquid state becomes unstable. The kinetics of the decay of such unstable states is analyzed in terms of the diffusion of voids.

PACS: 61.20.Gy, 61.25.Bi, 61.43.Fs, 64.70.Dv

1. INTRODUCTION

A phase transition corresponds to a transition between different aggregate states; for a first-order phase transition, the internal energy of a bulk system changes discontinuously as the temperature varies and the pressure is constant [1–3]. In contrast to this, a chemical transition, i.e., a transition between two limiting chemical states of a substance, occurs throughout some temperature range, with a shifting equilibrium ratio of the species, when conducted at a constant pressure. This principal difference between the phase and chemical transformations is lost for systems consisting of a finite number of atoms—notably, clusters [4–10]. Computer simulations of phase transitions in clusters [4–10] reveal some peculiarities of this phenomenon, in particular, the coexistence of the phases throughout some temperature range. From general considerations, one can infer that this range has sharp upper and lower bounds, which we may call the «melting limit» T_m and the «freezing limit» T_f . The range between T_f and

T_m can remain or shrink to zero as the number of particles N in the cluster grows very large. However in either case, the observable effect of increasing N is to make the range of the apparent coexistence shrink to a single temperature T_{eq} at which the free energies and mean chemical potentials of the two forms are equal. Away from this temperature, the thermodynamically unfavored phase can be present in observable amounts for relatively small N , but as N increases, the unfavored phase becomes so unfavored that the amounts or frequencies of its appearance become unobservably small. Because of the observability of unfavored phases for small systems, the transitions or phase changes between aggregate states are very similar to those between chemical states such as chemical isomers.

The study of phase transitions in clusters [4–10], especially focusing on their microscopic nature, has given us a deepened understanding of the nature of phase transitions for bulk systems. Analyzing the phase and chemical transformations in bulk systems from the microscopic standpoint, one can find both common and different features of these phenomena. Such an analysis is the goal of this paper. We are guided by the simplest

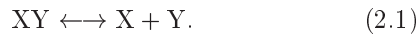
*E-mail: smirnov@orc.ru

cases for this analysis.

We compare the solid–liquid phase transition for a system of atoms bound by a pair interaction with the simple chemical transformations, ionization and dissociation. This comparison allows us to establish the common and different features of the phase and chemical transitions from the microscopic standpoint. The microscopic interpretation allows us to expand our understanding of the phase transition.

2. CHEMICAL EQUILIBRIUM AND TRANSFORMATIONS

We first consider the simplest chemical equilibria, in which a gaseous system consists of particles XY at low temperatures that dissociate into X and Y at high temperatures, and the chemical equilibrium therefore has the form



For the ionization equilibrium, we use this form and consider X to be an ion (A^+) and Y an electron (e), in which case the ionization equilibrium is



In parallel, we consider the dissociation equilibrium, in which the composite particles XY are dimer molecules and the dissociation equilibrium has the form



We use the simplest formulas for these equilibria. For the ionization equilibrium, the number densities of electrons N_e , ions N_i , and atoms N_a are related by the Saha equation [11, 12]

$$\frac{N_e N_i}{N_a} = \frac{g_e g_i}{g_a} \left(\frac{m_e T_e}{2\pi\hbar^2} \right)^{3/2} \exp\left(-\frac{J}{T_e}\right), \quad (2.4)$$

where m_e and T_e are the mass and temperature of electrons and g_e , g_i , and g_a are the statistical weights of the electron ($g_e = 2$), the ion, and the atom electronic states. Introducing the probabilities for an electron to be free $w_e = N_e/N$ or to be bound in an atom $w_a = N_a/N$ (where $N = N_e + N_a$ is the total number density of free and bound electrons, and hence, $w_e + w_a = 1$), we represent Saha formula (2.3) for a quasineutral plasma with $N_e = N_i$ as

$$\frac{w_e^2}{w_a} = g \exp\left(-\frac{J}{T_e}\right), \quad (2.5)$$

where the statistical weight g of free electron states is

$$g = \frac{1}{N} \frac{g_e g_i}{g_a} \left(\frac{m_e T_e}{2\pi\hbar^2} \right)^{3/2}. \quad (2.6)$$

In general, the statistical weight of free, continuum states is the ratio of the typical atomic number density in the condensed phase to the density of free atoms in the gas phase, and hence, this value is large. Therefore, the value $1/\ln g$ is a small parameter of the theory, because we consider transitions between free and bound states; these transitions occur in a relatively narrow range of temperatures due to a small value of this parameter. We note that we deal with an ensemble consisting of a sufficiently large number of particles to allow us to neglect the fluctuations.

We now determine the temperature width for this transition. We define the electron temperature for the ionization transition T_{ion} as the temperature for which $w_e(T_{ion}) = 1/2$. To be precise, we define the temperature range ΔT of the transition from atoms to electrons and ions such that the value w_e varies in this region from $1/4$ up to $3/4$. Hence, we have

$$\Delta T = \frac{T_{ion}^2}{J} \ln 27, \quad (2.7)$$

and a small parameter in this case is

$$T_{ion}/J = 1/\ln g.$$

In particular, under conditions of Fig. 1, Eq. (2.7) gives

$$\Delta T/T_{ion} = 0.3.$$

Using the same expressions for the probabilities of free and bound states, we have for the dissociation equilibrium

$$\frac{w_a^2}{w_m} = g \exp\left(-\frac{D}{T_e}\right), \quad (2.8)$$

where w_a is the probability for an atom to be free and w_m is the probability for an atom to be bound in the dimer molecule; D is the dissociation energy of the molecule. In contrast to the ionization equilibrium, where the probability of excited atom states is small, excited rotational and vibrational molecule states are taken into account in Eq. (2.8). But the structure of this formula is the same as for the ionization equilibrium. Figures 1 and 2 give some examples of the ionization and dissociation equilibria. The width of the transition between free and bound states in the temperature scale is determined by the small parameter $1/\ln g$ and decreases as the number density of particles decreases.

As a result of renormalization, we can infer from Eq. (2.5) the respective partition functions of free and bound electron states Z_e and Z_a . For the ionization equilibrium, we then have

$$\frac{Z_e^2}{Z_a} = g \exp\left(-\frac{J}{T_e}\right). \quad (2.9)$$

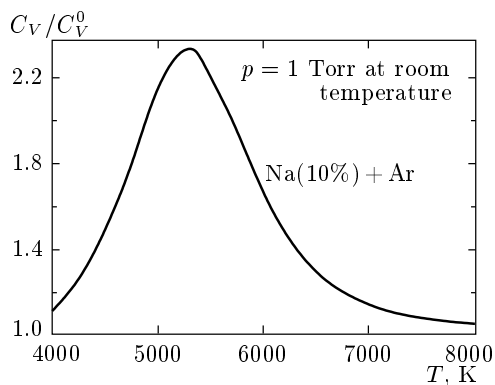


Fig. 1. The specific heat capacity of argon with a sodium admixture in the temperature range of the sodium ionization transition. The concentration of sodium atoms is equal to 10% and the number density of argon atoms corresponds to the pressure 1 Torr at room temperature

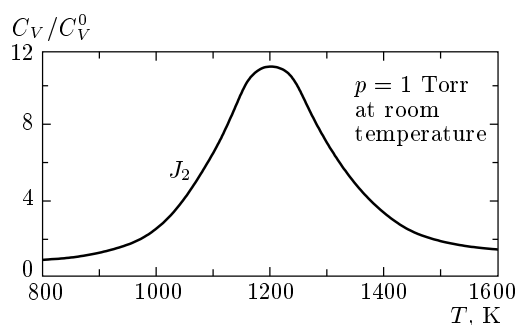


Fig. 2. The specific heat capacity of iodine J_2 in the range of the dissociation transition if the iodine number density corresponds to the pressure 1 Torr at room temperature

We obtain a corresponding relation for the dissociation equilibrium. These formulas can be used for the analysis of statistics of chemical equilibria.

We now determine the partial partition function for the ionization equilibrium that corresponds to a given number of free electrons at a certain temperature. An equivalent result appears for the dissociation equilibrium. If the total number of nuclei in the system is n and the number of ionized atoms is m , the probability of this event is determined by the Poisson formula

$$W_{nm} = C_n^m w_e^m w_a^{n-m} = C_n^m w_e^m (1 - w_e)^{n-m}, \quad (2.10)$$

where the ratio between w_e and w_a (with $w_e + w_a = 1$) is given by Eq. (2.5). The partition function Z_{nm} of the system with a given number of free and bound electrons is proportional to this value, and we take these values to be identical for simplicity. We note that formation

of m free electrons in this system corresponds to the excitation energy

$$m(J + 3T_e/2) \approx mJ.$$

For a large number of free and bound electrons in the system, i.e., $m \gg 1$ and $n \gg 1$, the partition function Z_{nm} has a sharp maximum as a function of m : near the maximum $m = m_0$, it has the form

$$Z_{nm} = Z_0 \exp \left[-\alpha (m - m_0)^2 \right], \quad (2.11)$$

and in accordance with the above relations, we have

$$m_0 = nw_e, \quad \alpha = \frac{1}{2m_0} \frac{n}{n - m_0}. \quad (2.12)$$

From this expression, we see that the partition function has a narrow maximum in the range of the number of broken bonds $\Delta m \sim \sqrt{n}$ if $m_0 \sim n$, and the relative maximum width $\Delta m/m_0$ tends to zero as $1/\sqrt{n}$ when the number of atoms tends to infinity.

3. CONFIGURATION EXCITATION OF A SYSTEM OF BOUND ATOMS

It follows from the above analysis that as a function of the excitation energy, the partition function is characterized by one maximum. In contrast to this, the partition function for the solid–liquid phase equilibrium has two maxima, and each maximum corresponds to a certain aggregate state. Below we consider, from this standpoint, the solid–liquid phase transition for condensed rare gases when the interaction between nearest neighbors dominates. We use measured parameters of the aggregate states of condensed rare gases near their triple points and consider a condensed rare gas as a system of bound atoms with short-range interactions, i.e., assume that interactions between nearest neighbors give the main contribution to the constitutive parameters of such systems. The reduced parameters of condensed rare gases are expressed through the parameters of the pair interaction potential of these atoms, which are known well [13–16]; this information is based on the parameters of diatomic molecules, condensed and dense rare gases and collision parameters of pairs of atoms. Next, the classical character of the atomic motion in condensed systems of Ne, Ar, Kr, and Xe, together with the short-range character of the interactions of atoms in these systems, allows us to use a scaling analysis to express bulk parameters of these systems through parameters of the interaction potential of two atoms. Simplifying this operation, we choose the parameters

of the pair interaction potential of these atoms as D , the depth of the potential well, and R_e , the equilibrium distance between atoms of the diatomic molecule. Adding to these parameters the atom mass m , we can express the physical value of any dimensioned property through the three parameters m , R_e , and D . The degree of coincidence of the reduced physical parameters for different rare gases then determines the accuracy of such a scaling law for real systems; for real rare gases, this measure of accuracy is several percent.

The analysis of parameters of the solid rare gases shows a small contribution of a long-range interaction. Indeed, the ratio of the distance a between nearest atoms in the solid rare gases at zero temperature to the equilibrium distance between atoms of the corresponding diatomic, averaged over all the stable rare gases, is [17–19]

$$a/R_e = 1.005 \pm 0.013,$$

and the reduced sublimation energy ε_{sub} of solid rare gases is 6.4 ± 0.2 per atom. For a system of bound atoms with only the nearest-neighbor interactions, these values are equal to 1 and 6 respectively, whereas for a system of atoms with the Lennard–Jones interactions, for which there is a long-range contribution to physical parameters of the system, the respective values are equal to 0.97 and 8.41 [20]. This shows that condensed rare gases are close to systems of atoms with the interaction between nearest neighbors only, and the error from this assumption is less than 10% for any parameter.

Taking real condensed rare gases as a system of bound atoms with a short-range interaction (i.e., the interaction between nearest neighbors only), we obtain additional information about this system on the basis of parameters of condensed rare gases. In particular, Table 1 contains the reduced parameters of the phase transition of this system near the triple point. In this Table, T_{tr} and p_{tr} are the temperature and pressure at the triple point, ΔH_{fus} and ΔS_{fus} are the fusion energy and the entropy change per atom as a result of the phase transition, ρ_{sol} and ρ_{liq} are the density of the solid and liquid rare gases at the triple point, and $\rho(0)$ is this value at zero temperature; the specific volume per atom for the solid and liquid states are denoted as V_0 and V_{liq} , respectively. In addition, the equilibrium vapor pressure p above the solid and liquid surfaces is given by the respective formula

$$p = p_{sol} \exp\left(-\frac{\varepsilon_{sol}}{T}\right), \quad p = p_{liq} \exp\left(-\frac{\varepsilon_{liq}}{T}\right), \quad (3.1)$$

where the parameters ε_{sol} and ε_{liq} characterize the binding energies per atom for the solid and liquid states

Table 1. Reduced average parameters of condensed rare gases at the triple point [17–10]

Reduced value	Average quantity
T_{tr}/D	0.579 ± 0.007
$p_{tr}R_e^3/D, 10^{-3}$	1.9 ± 0.2
$\Delta H_{fus}/D$	0.98 ± 0.02
ΔS_{fus}	1.68 ± 0.03
$p_{tr}\Delta V/\Delta H_{fus}, 10^{-4}$	2.2 ± 0.4
ε_{sub}/D	6.4 ± 0.2
$\rho(0)R_e^3/\sqrt{2}$	1.01 ± 0.04
$\rho_{sol}R_e^3/\sqrt{2}$	0.92 ± 0.02
$\rho_{liq}R_e^3/\sqrt{2}$	0.80 ± 0.02
V_{liq}/V_0	1.153 ± 0.006
ε_{ev}/D	5.4 ± 0.2
$p_{sol}R_e^3/D$	110 ± 20
$p_{liq}R_e^3/D$	25 ± 4
ε_{liq}/D	5.5 ± 0.1
T_{cr}/D	1.04 ± 0.02

of this system, to within the accuracy of the thermal energy at the melting point. The parameters of Eq. (3.1) are given in Table 1.

It follows from the data in Table 1 that the mechanical work $p_{tr}\Delta V$ during the phase transition of a real rare gas near the triple point is small compared to the change ΔH_{fus} of the internal energy of the constituent atoms. This simplifies the analysis and allows us to neglect the expansion of the system of bound atoms during the phase transition, and hence, to treat this process as a function of only one variable. Below, we consider the temperature range of the melting point where the criterion

$$\Delta H_{fus} \gg p\Delta V \quad (3.2)$$

is satisfied. Here, p is the pressure on the melting curve and ΔV is the increase of the specific volume. In this temperature range, the attractive part of the pair interaction potential of atoms is responsible for the behavior of this system of atoms, and it is not necessary to explicitly account for the external pressure because that would be very small compared to the attraction forces

between the interacting atoms. This criterion is valid under the condition

$$p \ll \frac{D}{R_e^3}. \quad (3.3)$$

Equation (3.1) and the data in Table 1 imply that these criteria are valid at least at temperatures

$$T < T_{cr}, \quad (3.4)$$

where T_{cr} is the critical temperature for the liquid–gas transition (see Table 1). We note that at high external pressures, the repulsive part of the pair interaction potential of atoms is important for the phase transition and the mechanical work $p\Delta V$ makes a considerable contribution to the fusion energy.

We now analyze the excitation of a system of many bound atoms with a pair interaction in the case where the interaction between nearest neighbors dominates. Computer simulations of clusters, which are systems of such bonded atoms and have completed shells, show the complex character of the phase transition. At a certain degree of excitation, atoms of filled shells move out of those shells to the cluster surface; they float on it, albeit with somewhat hindered motion, and then return, typically exchanging roles with other atoms coming out of the surface layer [21, 22]. These transitions are easiest for the outermost shell, but are possible for others beneath, and in some range of temperatures one can thus construct several calorimetric curves [23], each describing the excitation of a particular shell. Evidently, when a cluster becomes very large, one can extract the surface excitation and the bulk (internal) excitation in this way. Although we here draw from the experience of phase transitions in clusters, in order to simplify this analysis, we restrict the further discussion to internal excitations only, and therefore consider infinite clusters or bulk systems of bound atoms.

We note two types of excitations in a bulk system of bound atoms. The first deals with the excitation of vibrations or phonons; this excitation is identical in principle for the solid and liquid states, apart from the regular character of excitations of a periodic lattice. The excitation of the other type, the configuration excitation, corresponds to a change in the atomic positions. When this excitation is small, it can be characterized by the change in the number of vacancies inside the crystal lattice. These vacancies result from removal of atoms from sites of the crystal lattice to positions outside. When the number of vacancies becomes large, such that neighboring vacancies border, these vacancies transform into voids [24], and the energy of formation of

an individual void, as well as its volume, depends on the degree of the configuration excitation. We assume the excitations of these two types to be independent and analyze the configuration excitation, which is responsible for the phase transition as a result of formation of voids inside the system.

Considering the configuration excitation to be un-equilibrium with respect to the thermal motion of atoms, we use a simple model for this excitation [25–27]. We prepare an excited state as follows. In a crystal consisting of $n + v$ atoms, we create v vacancies inside by removing v atoms to the outside. Then v , the number of vacancies formed, characterizes the excitation degree of this system. In the second stage of the evolution, this system relaxes such that it shrinks, and its internal energy typically (but not necessarily) drops. We characterize the degree of the configuration excitation of this system by the number of voids v , which coincides with the number of interior vacant sites. Of course, in contrast to a vacancy, an individual void varies its form and volume in time; we consider an individual void in terms of its average form and volume. We use statistical parameters for each void, characterizing it by a certain energy ε_v of its formation and the statistical weight g_v . Thus, we describe the degree of the configuration excitation of the system by the number of voids that are initially isolated vacancies. In this manner, we consider an excitation as a gas of noninteracting voids that are identical on average, whereas the parameters of an individual void depend on the degree of excitation.

The statistical model under consideration involves averaging over atomic positions in a system of interacting atoms. If we restrict the treatment to interactions between nearest neighbors only, we can express the excitation energy through the average number of the nearest neighbors n_c for any internal atom. The mean binding energy per atom is then given by

$$\varepsilon = Dn_c/2,$$

where D is the binding energy per individual bond and the average volume per atom is

$$V = 12V_0/n_c,$$

where the specific volume V_0 is that based on the solid state. From this, we have

$$V = V_0 \frac{\varepsilon_{sub}}{\varepsilon} = V_0 \frac{n\varepsilon_{sub}}{\varepsilon_{sub} - \varepsilon_v v/n}, \quad (3.5)$$

where ε_v is the energy of formation of one elementary void and ε_{sub} is the binding energy per atom for the

solid state. In particular, this implies that for the liquid state,

$$\xi_{liq} \equiv \frac{V_0}{V} \frac{\varepsilon_{sub}}{\varepsilon_{sub} - \Delta H_{fus}} = 1, \quad (3.6)$$

and the statistical average of this parameter over real rare gases gives

$$\xi_{liq} = 1.024 \pm 0.006,$$

and Eq. (3.2) is therefore valid within the accuracy of 3%. Evidently, the error in ξ_{liq} is related to the accuracy of using the mean-field approximation.

Considering the liquid–solid phase transition as a result of the formation of voids, we construct the partition function of a void gas as

$$Z(v) = C_{n+v}^v g_v^v \exp\left(-\frac{v\varepsilon_v}{T}\right), \quad (3.7)$$

where ε_v is the energy of formation of an individual void, g_v is the statistical weight of a void, and these parameters depend on the parameter $x = v/n$. Assuming voids to be independent, we define the energy of the formation of an individual void as

$$\varepsilon_v = \varepsilon_0 - U\left(\frac{v}{n}\right), \quad (3.8)$$

where U is the effective interaction potential of voids, ε_0 is the energy of the formation of a vacancy in the crystal as a result of removing an internal atom to the surface, i.e., when $v = 0$ ($\varepsilon_0 = 6D$ in the case of the interaction between nearest neighbors only). We take the statistical weight of an individual void to have the form [26, 27]

$$g = 1 + a\frac{v}{n}, \quad a \gg 1. \quad (3.9)$$

For the effective interaction potential, we use [26, 27]

$$\begin{aligned} U\left(\frac{v}{n}\right) &= \varepsilon_0 \left[\exp\left(-\frac{\alpha n}{v}\right) - \exp\left(-k\frac{\alpha n}{v}\right) \right] = \\ &= \varepsilon_0 u\left(\frac{v}{n}\right), \end{aligned} \quad (3.10)$$

$$u(x) = \exp\left(-\frac{\alpha}{x}\right) - \exp\left(-k\frac{\alpha}{x}\right),$$

where α and k are parameters. These relations imply that as the unoccupied space inside the system increases, the statistical weight per atom increases, and the energy of the formation of new vacancies decreases. It then follows that the reduced logarithm of the partition function is given by

$$\begin{aligned} \frac{\ln Z(v)}{n} &= x \ln(1 + ax) + \ln(1 + x) + \\ &+ x \ln\left(1 + \frac{1}{x}\right) - x\frac{\varepsilon_0}{T} [1 - u(x)], \quad x = \frac{v}{n}. \end{aligned} \quad (3.11)$$

Table 2. Mean parameters of condensed rare gases at the triple point

Value	Average quantity
α	0.13 ± 0.01
k	4.8 ± 0.2
v_{liq}/n	0.31 ± 0.01
a	65 ± 15
$U(v_{liq}/n)/D$	3.3 ± 0.2
$U(v_{min}/n)/D$	1.3 ± 0.1
$-\ln Z((v_{min}/n)/n)$	0.39 ± 0.02

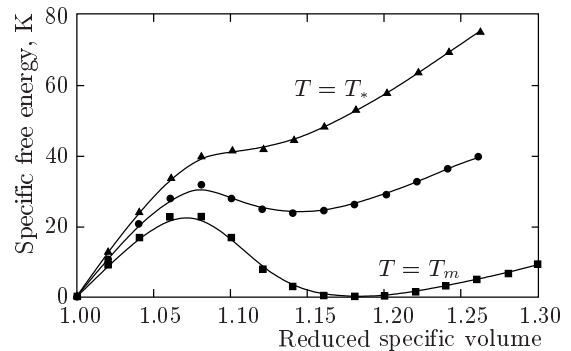


Fig. 3. The dependence of the specific free energy of condensed rare gases on the reduced volume per one atom. The right minimum corresponds to the liquid state; at $T = T_*$, the liquid state becomes unstable

The use of the phase transition parameters for condensed rare gases at their triple points together with this expression for the partition function allows us to find the parameters of this model [25–27]. We note that the complex form (3.6) of the effective interaction potential of voids is related to a bimodal form of the partition function that cannot be realized at $k = \infty$. The parameters of this model averaged over the stable rare gases are given in Table 2 [26, 27].

One can continue the partition function of a system of bound atoms to the range of low temperatures, where the liquid state of the bulk is a metastable aggregate state. Figure 3 shows the dependence of the specific free energy

$$F = -T \ln Z$$

on the specific volume and is based on Eqs. (3.5) and (3.7)–(3.10); the mechanical work as a result of the

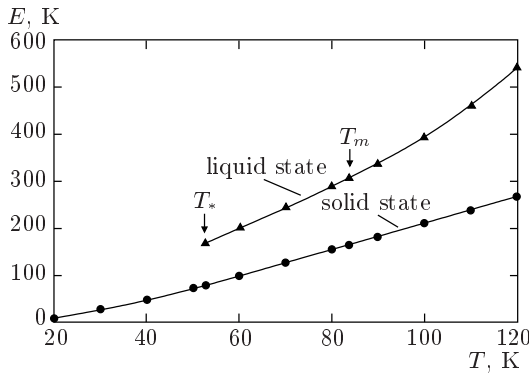


Fig. 4. Caloric curves for argon — the temperature dependences of the internal energy of aggregate states. The solid caloric curve is given by Eq. (4.1) and the caloric curve is given by Eq. (4.3)

phase transition is neglected in accordance with criteria (3.3) and (3.4). The first (left) maxima of these curves in Fig. 3 at low excitation energy corresponds to the solid state; the second correspond to the liquid state. We use Eq. (3.7) for the specific partition function and the relations between the volume per one atom V , the specific excitation energy $v\varepsilon_v/n$, and the relative number of voids v/n . It follows from Fig. 3 that below the freezing limit $T_* = 0.36D$, the liquid maximum of the partition function disappears and the liquid state becomes unstable.

4. THE CALORIC CURVE OF CONDENSED RARE GASES AND THE RATE OF EQUILIBRATION

Thus, neglecting the surface configuration excitation of large clusters of rare gases, we restrict our description to two aggregate states that correspond to the solid and liquid states of a bulk system. Figure 4 gives the caloric curves for these states. Each caloric curve is the temperature dependence of the specific internal energy of the isothermal system of bound atoms. We take the excitation energy as a sum of the phonon excitation energy and the configuration excitation energy. The phonon contribution to the excitation energy per atom is given by [11]

$$E_{ph} = 3Td \left(\frac{\Theta_D}{T} \right), \quad (4.1)$$

where

$$d(x) = \frac{3}{x^3} \int_0^x \frac{z^3 dz}{\exp(z) - 1} \quad (4.2)$$

is the Debye function; the Debye temperature Θ_D does not conform to the scaling law. Figure 4 corresponds to argon, for which we take [20, 28] $\Theta_D \approx 90$ K. The specific energy of the configuration excitation is taken as $v\varepsilon_v/n$ for the liquid state and is zero for the solid state, and therefore, the total specific internal energy of the liquid state is

$$E_{liq} = 3Td \left(\frac{\Theta_D}{T} \right) + \frac{v}{n} \varepsilon_{vliq}, \quad (4.3)$$

and the second term is absent for the solid state. Next, the liquid caloric curve terminates at the freezing limit T_* where the liquid maximum of the free energy disappears (see Fig. 3). In the same manner, the solid caloric curve terminates at high temperatures in this formulation. Because the critical temperature of the solid state is sufficiently high such that the mechanical work of solid–liquid transitions cannot be neglected, it would be incorrect to discuss the high-temperature range of the caloric curve within this framework. Because the scaling law is invalid for the phonon excitation energies, we specifically analyze the parameters of argon in what follows.

We note the principal difference in the construction of caloric curves for clusters and for bulk systems. For clusters, the coexistence of the solid and liquid phases is possible in some temperature range where the probability of the location of a cluster in each aggregate state is nonnegligible. Hence, assuming that the time intervals between transitions from one aggregate state to another is long compared to the observation time and that the times required for the transitions are brief on the same scale, we terminate the caloric curve of each state at a temperature at which the probability of observing the cluster in this state becomes small. (More rigorously, we could terminate where the local minimum in the free energy of that form disappears.) For large clusters or a bulk system, this probability of the observation of the unfavored phase is very, very small, even in the vicinity of the melting point, but a typical dwell time in one phase may be long, even infinite, precisely at the melting point, if the cluster is macroscopic. Hence, constructing the caloric curve in Fig. 4 for argon, we suppose the mean dwell time in the liquid state to be sufficiently long. The true low-temperature termination of the liquid caloric curve means that at even lower temperatures, the metastable liquid state does not exist. In addition, Fig. 5 gives the specific volume of the argon liquid state; the argon fusion energy for the solid–liquid phase transition is represented in Fig. 6. In accordance with criteria (3.3)–(3.5), our

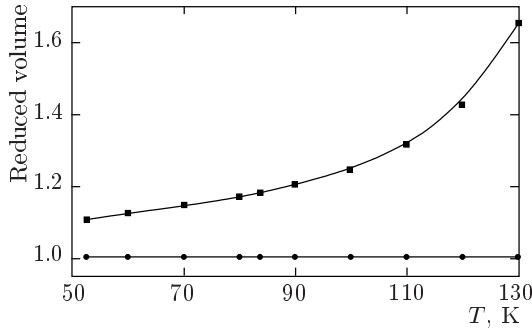


Fig. 5. The volume per atom for solid and liquid argon states in neglecting the anharmonicity of the atom motion

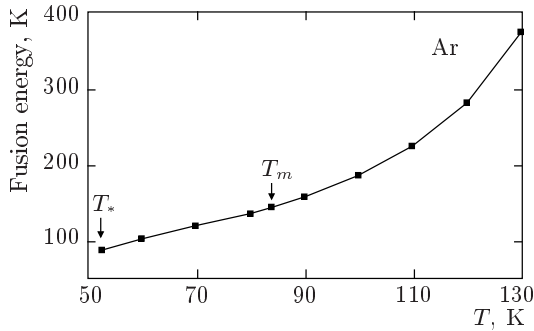


Fig. 6. The fusion energy for the solid–liquid phase transition in argon

treatment is restricted to a range of temperatures that are not too high.

For a bulk system, the decay of the liquid state below the melting point is determined by fluctuations due to nonuniformities in the void distribution. This also occurs for small clusters. For very large clusters or bulk systems, we neglect these fluctuations, and metastable liquid states can therefore live very long in the absence of external perturbations. Below the freezing limit, the decay of an unstable liquid state results from the diffusion of voids to the boundary of the system; below, we briefly analyze this process.

Because the diffusion process has an activation character, it slows down with a temperature decrease and stops at sufficiently low temperatures. Because the voids move by diffusion, the rate of this process depends on the geometry of the system. We consider atoms to be bonded with a substratum, and bound atoms to form a film on the substratum surface. (The substratum may be another layer of the same material.) If the film thickness is l , the typical time of a void de-

parture outside the film is of the order l^2/D_{dif} , where D_{dif} is the diffusion coefficient of voids inside the film. Because a displacement of voids is determined by the inverse displacement of atoms, the diffusion coefficient of voids is

$$D_{dif} \sim \omega_D a^2 \exp\left(-\frac{E_a}{T}\right), \quad (4.4)$$

where $\omega_D = \Theta_D/\hbar$ is the Debye frequency, a is the lattice constant, T is a current temperature, and E_a is the activation energy for the atomic displacement, which depends on the relative number of voids or vacancies inside the system. We assume that the heat transport proceeds more effectively than the process of void diffusion because of the activation character of the last process, i.e., the criterion

$$D_{dif} \ll \chi, \quad (4.5)$$

is satisfied, where χ is the thermal diffusivity coefficient.

The activation energy drops if the relative number of voids drops. Evidently, the «frozen» temperature (an analogue of the glassy temperature [30]) is determined by the condition

$$\int \frac{D_{dif}}{l^2} dt \sim 1. \quad (4.6)$$

Assuming the temperature variation rate dT/dt to be constant, we obtain from Eqs. (4.5) and (4.4) that

$$\frac{\omega_D a^2}{l^2} \exp\left(-\frac{E_a}{T_f}\right) \frac{T_f^2}{E_a \frac{dT}{dt}} \sim 1, \quad (4.7)$$

where T_f is the temperature below which voids are frozen, and the activation energy $E_a \gg T_f$ corresponds to a frozen relative number of voids.

The activation energy of this process increases as the number of voids decreases. Below, we consider this transition in the limit in which the atoms form a crystal lattice, and even the nearest vacancies do not border each other. We take a face-centered cubic lattice for the solid state of the system of bound atoms. The transition of a vacancy from one lattice site to a neighboring one is similar to the transition of an atom next to a vacancy to the vacancy site. For simplicity, we fix other atoms in the sites of the crystal lattice. To make the transition to a neighboring site, a test atom must overcome a barrier; from symmetry considerations, the barrier height is the difference of the total interaction potentials of atoms with the test atom located in a site

of the crystal lattice and halfway between two neighboring vacancies. If we introduce the pair interaction potential of atoms $U(R)$ at the distance R between them, we obtain the barrier height

$$E_a = -11U(a) - 2U(\sqrt{2}a) - 4U(\sqrt{3}a) - U(2a) + 4U\left(\frac{\sqrt{3}}{2}a\right) + 4U\left(\frac{\sqrt{5}}{2}a\right) + 8U\left(\frac{\sqrt{7}}{2}a\right) + 2U\left(\frac{3}{2}a\right). \quad (4.8)$$

We account for the interaction of a transiting atom with the nearest neighbors as it passes from the initial to the final atom position; a is the distance between nearest neighbors of the lattice.

In particular, we use the Lennard–Jones interaction potential between atoms

$$U(R) = D \left[\left(\frac{R_e}{R} \right)^{12} - 2 \left(\frac{R_e}{R} \right)^6 \right], \quad (4.9)$$

where R_e is the equilibrium distance between atoms for a classical diatomic molecule and D is its dissociation energy. In this case, we have

$$E_a = 9.2D. \quad (4.10)$$

For the Morse interaction potential

$$U(R) = D [\exp(-2\alpha(R - R_e)) - 2 \exp(\alpha(R - R_e))] \quad (4.11)$$

and the Morse parameter $\alpha = 6/R_e$ (making the potential as similar to the Lennard–Jones one as possible), we have

$$E_a = 8.2D. \quad (4.12)$$

We note that both interaction potentials are characterized by identical dissociation energies D of the diatomic molecule and identical second derivatives of the interaction potentials at their equilibrium distances,

$$U''(R_e) = 72/R_e^2.$$

If we restrict the interactions to those between nearest neighbors of the crystal lattice, then $a = R_e$. These results can be used to obtain an upper limit for the activation energy of the transition under consideration. The criterion of validity of Eqs. (4.11) and (4.12) is such that neighboring voids are individual vacancies at the crystal lattice sites, i.e., $v \ll n/12$.

We now analyze the character of the frozen process under the conditions of the specific experiment [29, 30],

when the thickness of the argon film on the copper target is $0.1 \mu\text{m}$ and the cooling rate is 2 K/min . In accordance with Eq. (4.7), voids are frozen if $E_a/T_f \approx 14$. If the decay of an unstable state resulting from an irreversible transport of voids starts from the temperature $T_* = 52 \text{ K}$, some fraction of the voids diffuses to the outside under the given conditions, until the activation energy of the void diffusion process reaches the value

$$E_a = 14T_* \approx 5D.$$

Because this value is less than the activation energy (4.10) and (4.12) for the diffusion of vacancies in the crystal, some of the voids are frozen by this cooling process. Thus, it follows from the above estimate that a system of bound atoms is characterized by a nonequilibrium number of voids or vacancies that are caught and frozen at low temperatures, and this number depends on the rate of cooling of this system.

5. CONCLUSION

Although there is no difference in the forms of the temperature dependence of some physical parameters for systems of a finite number of bound atoms in the cases of chemical transformations and phase transitions, these phenomena are different in principle due to the different dependences of the corresponding partition functions on the number of elementary excitations or the excitation energy. For chemical transformations, the partition function has a sharp maximum at the average number of excitations at a given temperature, and this maximum tends to infinity as the number of excitations tends to infinity. The temperature variation leads to a smooth transition from one chemical state of the system to the other. For the phase transition of a large system, when surface excitations are not important, the partition function has two maxima as a function of the number of elementary configuration excitations; these maxima correspond, e.g., to the solid and the liquid. The liquid state is characterized by a freezing limit below which the liquid maximum disappears. Quenching the configuration excitations in a large system of interacting atoms results in a transport of voids to the boundaries of the system or from them. The character of the void transport process determines the state of this system of bound atoms after its cooling.

This paper is supported in part by the RFBR (grant 99-02-16094) and by the National Science Foundation.

REFERENCES

1. R. Brout, *Phase Transitions*, Benjamin Inc., New York (1965).
2. E. Stanley, *Introduction to Phase Transitions and Critical Phenomena*, Oxford, Univ. Press, New York (1971).
3. A. R. Ubbelohde, *The Molten State of Matter*, Wiley, Chichester (1978).
4. R. S. Berry, J. Jellinek, and G. Natanson, *Phys. Rev. A* **30**, 919 (1984).
5. R. S. Berry, J. Jellinek, and G. Natanson, *Chem. Phys. Lett.* **107**, 277 (1984).
6. J. Jellinek, T. L. Beck, and R. S. Berry, *J. Chem. Phys.* **84**, 2783 (1986).
7. R. S. Berry, T. L. Beck, H. L. Davis, and J. Jellinek, *Adv. Chem. Phys.* **90**, 75 (1988).
8. D. J. Wales and R. S. Berry, *J. Chem. Phys.* **92**, 4283 (1990).
9. R. S. Berry, *Nature* **393**, 238 (1998).
10. R. S. Berry, in: *Theory of Atomic and Molecular Clusters*, ed. by J. Jellinek, Springer, Berlin (1999), p. 1.
11. L. D. Landau and E. M. Lifshitz, *Statistical Physics*, Vol. I, Pergamon Press, Oxford (1980).
12. B. M. Smirnov, *Physics of Ionized Gases*, Wiley, New York (2001).
13. R. A. Aziz and M. J. Slaman, *Chem. Phys.* **130**, 187 (1989).
14. R. A. Aziz and M. J. Slaman, *J. Chem. Phys.* **92**, 1030 (1990).
15. A. K. Dham, A. R. Allnatt, W. J. Meath, and R. A. Aziz, *Mol. Phys.* **67** 1291 (1989).
16. A. K. Dham, W. J. Meath, A. R. Allnatt, R. A. Aziz, and M. J. Slaman, *Chem. Phys.* **142**, 173 (1990).
17. B. M. Smirnov, *Phys. Uspekhi* **35**, 1052 (1992).
18. B. M. Smirnov, *Phys. Uspekhi* **37**, 1079 (1994).
19. B. M. Smirnov, *Clusters and Small Particles in Gases and Plasmas*, Springer, New York (2000).
20. Ch. Kittel, *Introduction to Solid State Physics*, 6th Edition, Wiley, New York (1986).
21. H. P. Cheng and R. S. Berry, *Phys. Rev. A* **45**, 7969 (1992).
22. H. P. Cheng, X. Li, R. L. Whetten, and R. S. Berry, *Phys. Rev. A* **46**, 791 (1992).
23. R. E. Kunz and R. S. Berry, *Phys. Rev. E* **49**, 1895 (1994).
24. H. Reiss, H. L. Frisch, and J. L. Lebowitz, *J. Chem. Phys.* **31**, 369 (1959).
25. B. M. Smirnov, *Phys. Scripta* **58**, 595 (1998).
26. B. M. Smirnov, *Inorg. Mater.* **35**, 562 (1999).
27. B. M. Smirnov, in: *Nucleation Theory and Applications*, ed. by J. W. R. Schmelzer, G. Röpke, and V. B. Priezhev, JINR, Dubna (1999), p. 355.
28. N. Schwenther, E. E. Koch, and J. Jortner, *Electronic Excitations in Condensed Rare Gases*, Springer, Berlin (1985).
29. A. Kouchi and T. Kuroda, *Jap. J. Appl. Phys.* **29**, 807 (1990).
30. I. Gutzow and J. Schmelzer, *The Vitreous State*, Springer, Berlin (1995).